Marine Chemistry 224 (2020) 103815

Contents lists available at ScienceDirect

Marine Chemistry

journal homepage: www.elsevier.com/locate/marchem

Natural Fe-binding organic ligands in Fram Strait and over the northeast Greenland shelf

Indah Ardiningsih[a,*], Stephan Krisch[b], Pablo Lodeiro[b], Gert-Jan Reichart[a,c], Eric P. Achterberg[b], Martha Gledhill[b], Rob Middag[a], Loes J.A. Gerringa[a]

[a] Royal Netherlands Institute for Sea Research (NIOZ), Department of Ocean Systems, University of Utrecht, PO Box 59, 1790 AB Den Burg, the Netherlands
[b] GEOMAR Helmholtz Centre for Ocean Research Kiel, Wischhofstr.1-3, 24148, Kiel, Germany
[c] Earth and Geoscience Department, University of Utrecht, Utrecht, the Netherlands

ARTICLE INFO

Keywords:
Fe-binding ligands
Iron speciation
Fram Strait

ABSTRACT

There is a paucity of data on Fe-binding ligands in the Arctic Ocean. Here we investigate the distribution and chemical properties of natural Fe-binding ligands in Fram Strait and over the northeast Greenland shelf, shedding light on their potential sources and transport. Our results indicate that the main sources of organic ligands to surface waters of Fram Strait included primary productivity and supply from the Arctic Ocean. We calculated the mean total Fe-binding ligand concentration, [L_t], in Polar Surface Water from the western Fram Strait to be 1.65 ± 0.4 nM eq. Fe. This value is in between reported values for the Arctic and North Atlantic Oceans, confirming reports of north to south decreases in [L_t] from the Arctic Ocean. The differences between ligand sources in different biogeochemical provinces, resulted in distinctive ligand properties and distributions that are reflected in [L_t], binding strength (log $K'_{Fe'L}$) and competing strength (log $\alpha_{Fe'L}$) of ligands. Higher [L_t] was present near the Nioghalvfjerdsfjorden (79 N) Glacier terminus and in the Westwind Trough (median of [L_t] = 2.17 nM eq. Fe; log $K'_{Fe'L}$ = 12.3; log $\alpha_{Fe'L}$ = 3.4) than in the Norske Trough (median of [L_t] = 1.89 nM eq. Fe; log $K'_{Fe'L}$ = 12.8; log $\alpha_{Fe'L}$ = 3.8) and in Fram Strait (median of [L_t] = 1.38 nM eq. Fe; log $K'_{Fe'L}$ = 13; log $\alpha_{Fe'L}$ = 3.9). However, organic ligands near the 79 N Glacier terminus and in the Westwind Trough were weaker, and therefore less reactive than organic ligands in the Norske Trough and in Fram Strait. These weaker ligands, although more abundant than in the Fram Strait, reduce overall Fe solubility in waters transported from the 79N Glacier to Fram Strait. The lower ligand binding strength in the outflow results in a higher inorganic Fe concentration, [Fe′], which is more prone to precipitation and/or scavenging than Fe complexed with stronger ligands. Ongoing changes in the Arctic and sub-Arctic Oceans will influence both terrestrially derived and in-situ produced Fe-binding ligands, and therefore will have consequences for Fe solubility and availability to microbial populations and Fe cycling in Fram Strait.

1. Introduction

The Arctic region is undergoing rapid environmental changes (Gascard et al., 2008; IPCC, 2014), including permafrost (Schuur et al., 2015) and ice-sheet melt (Ekwurzel et al., 2001). The environmental alteration induced by climate changes will influence the biogeochemical cycle of many elements, including iron (Fe), an important micronutrient regulating the dynamics of primary productivity (Boyd et al., 2000; De Baar, 1990; Martin and Fitzwater, 1988; Rijkenberg et al., 2018). In the shelf-dominated Arctic Ocean, the Polar Surface Water (PSW) is strongly influenced by runoff from Eurasian rivers with waters reaching the central basin via the Transpolar Drift (TPD) (Gascard et al., 2008; Gordienko and Laktionov, 1969), and lateral transport over the shelf areas. The runoff introduces organic matter, fluvial sediment, and other terrigenous materials (Ekwurzel et al., 2001; Klunder et al., 2012; Measures, 1999). These materials contribute organic ligands of terrestrial origin, mainly humics (Laglera et al., 2019a; Slagter et al., 2019). The organic ligands stabilize Fe in the dissolved form, and prevent Fe from precipitating (Kuma et al., 1996; Millero et al., 2002), thereby enabling a substantial amount of dissolved-Fe (DFe) to be present in PSW (Klunder et al., 2012; Rijkenberg et al., 2018; Slagter et al., 2017). Determining the complexation of Fe with organic ligands is, thus, a crucial component of Fe biogeochemistry. The PSW, enriched in DFe bound to terrestrially derived organic ligands as well as ligands

* Corresponding author.
E-mail address: indah.ardiningsih@nioz.nl (I. Ardiningsih).

https://doi.org/10.1016/j.marchem.2020.103815
Received 6 December 2019; Received in revised form 25 April 2020; Accepted 27 April 2020
Available online 01 May 2020

produced in the Arctic Ocean, can be transported out of the central Arctic via Fram Strait (Laukert et al., 2017; Slagter et al., 2019), a main gateway for heat and water mass exchange between the Arctic Ocean and the Nordic Seas (Greenland Sea, Norwegian Sea and Iceland Sea) (Rudels et al., 2005; Rudels et al., 2015). In the vicinity of Fram Strait, the Nioghalvfjerdsfjorden (79 N) Glacier terminates on the northeast Greenland shelf, where the Norske Trough and Westwind Trough are located. The ongoing changes in the Arctic and sub-Arctic Oceans will influence the sources of Fe-binding organic ligands, and therefore have consequences for DFe supply and transport, particularly in Fram Strait. However, there is a paucity of data to comprehensively assess the effect of global climate change on the biogeochemical cycle of DFe as well as associated feedback mechanisms.

Iron is present at sub-nanomolar levels in oceanic water due to its low solubility and low supply rate (Liu and Millero, 2002), limiting primary productivity in approximately one third of the global ocean (Boyd et al., 2000; De Baar, 1990; Martin and Fitzwater, 1988; Rijkenberg et al., 2018). In seawater, DFe can exist in two different oxidation states, Fe(II) and Fe(III). The Fe(III) oxidation state dominates the chemical speciation of DFe around pH 8 in oxygenated waters, forming Fe oxy-hydroxides (Kuma et al., 1996). At the natural seawater pH, Fe oxy-hydroxides tend to undergo further hydrolysis, and are thus prone to precipitation. However, organic complexation by Fe-binding ligands shifts the equilibrium reaction away from Fe hydrolysis (Kuma et al., 1996; Millero et al., 2002), governing Fe solubility in seawater (Gledhill and Buck, 2012; Hunter and Boyd, 2007). Despite its importance in determining Fe solubility, Fe-binding ligand data is scarce, notably in ice-covered Arctic and subarctic regions.

To date, only a few studies have looked at Fe-binding ligands in the subarctic and Arctic Ocean. Thuróczy et al. (2011) presented the first dataset on Fe fractionation and organic chelation in the central Arctic. Recently, the terrestrial influence on organic ligands in surface waters of the Arctic Ocean was investigated (Slagter et al., 2017). The high concentrations of DFe (up to 4.4 nM) in PSW (Klunder et al., 2012; Rijkenberg et al., 2018) were facilitated by complexation with enhanced concentrations of organic ligands (Slagter et al., 2017). This surface DFe enhancement was a clear indication of a riverine contribution in the flow path of the TPD in the Arctic Ocean. The DFe and Fe-binding ligand concentrations were up to 4.5 and 1.7 times higher inside than outside the flow of the TPD, respectively, and ligands from terrestrial origin dominated the total ligand pool in the TPD (Laglera et al., 2019a). This indicates a transport of organic Fe-binding ligands via the TPD (Slagter et al., 2019), and these ligands are likely transported out of the Arctic Ocean towards Fram Strait.

The concentrations and conditional stability constants ($K'_{Fe'L}$) of Fe-binding ligands in seawater are typically determined by the electrochemical technique known as competitive ligand equilibration (CLE) – adsorptive cathodic stripping voltammetry (AdCSV). This technique is based on the competitive equilibrium between an added known ligand and natural ligands present in seawater (Abualhaija and van den Berg, 2014; Croot and Johansson, 2000; Gledhill and van den Berg, 1994; Rue and Bruland, 1995; van den Berg, 2006). A distribution of conditional stability constants is commonly used to classify Fe-binding ligand groups (Gledhill and Buck, 2012), although the boundaries between the groups are still indistinct and probably more gradual than first assumed. In short, three key groups are acknowledged, (i) strong Fe-binding siderophores (Mawji et al., 2008; Velasquez et al., 2016; Vraspir and Butler, 2009), (ii) relatively weak Fe-binding humic substances (Bundy et al., 2014; Laglera and van den Berg, 2009), and (iii) relatively weak Fe-binding microbially-excreted sugars such as polysaccharides or exopolymeric substances (Hassler et al., 2011). Siderophores are defined as low-molecular-weight organic compounds (< 1 kDa) secreted by prokaryotes as part of an Fe-uptake system (Mawji et al., 2008; Vraspir and Butler, 2009). Humic substances (HS) typically come from the degradation of organic matter; they have a strong terrestrial component in the Arctic and are substantially resistant to degradation (Calace et al., 2001; Laglera et al., 2019a; Laglera and van den Berg, 2009). However, marine HS can also be produced in situ by bacterial remineralization of biogenic particles (Burkhardt et al., 2014) and grazing (Decho and Gutierrez, 2017; Laglera et al., 2019b). Exopolymeric substances (EPS) are relatively labile macromolecules excreted by microbial cells during all life cycles of phytoplankton growth (Decho and Gutierrez, 2017). During an extreme bloom and following its termination, EPS can dominate from 1% to 50% of the dissolved organic carbon (DOC) pool (Orellana et al., 2003) and together with HS, can be a significant contributor of colloidal organic ligands (Batchelli et al., 2010; Hassler et al., 2011). As microbial exudates, EPS are expected to be produced abundantly up to micromolar levels in surface waters, also at the base of sea ice (Lannuzel et al., 2015), showing the potential to outcompete the stronger ligand group (Hassler et al., 2011). The classification of weak and strong ligand groups based on these three groups is challenging. For example, Slagter et al. (2019) concluded that HS, thought to be a weaker ligand group, can also contain relatively strong ligands (log $K'_{Fe'L}$ 11.5–12.6), whereas Norman et al. (2015) demonstrated that EPS could have strong binding stability constants as well (log $K'_{Fe'L} > 12$).

This study focuses on the distribution and chemical properties of natural Fe-binding ligands in Fram Strait and over the northeast Greenland shelf. Concentrations of dissolved and total dissolvable Fe of the same expedition (Krisch et al., submitted) are here combined with the distribution and chemical properties of natural Fe-binding ligands in Fram Strait and over the northeast Greenland shelf (77°N – 81°N and 20°W – 20°E), shedding light on their potential sources and transport and further elucidate the cycling of both Fe and Fe-binding ligands in the rapidly changing Fram Strait region.

2. Material and methods

2.1. Sampling

Samples were obtained during GEOTRACES expedition GN05 (PS100) on the German research vessel Polarstern during summer 2016. Seawater samples for trace metals and ligands were sampled between 22nd July and 1st September. Details about the cruise track, ice-cover and hydrographic data can be found in the expedition report (Kanzow, 2017).

A total of 10 stations were sampled as full depth profiles, 8–12 ligand samples per station in Fram Strait and 5–7 samples per station over the shelf. Conductivity, temperature, depth (CTD), oxygen and turbidity profiles were obtained using a titanium Seabird SBE 911plus on a trace metal clean rosette frame. The frame was equipped with 24 × 12 L Go-Flo bottles (Ocean Test Equipment) and seawater was collected following the sampling procedures as described by Cutter et al. (2010). Across Fram Strait, samples were collected from 4 different stations (1, 7, 14 and 26). Station 1 was located on the eastern side of Fram Strait close to the Svalbard archipelago, while stations 7, 14 and 26 were located towards the western side of Fram Strait (Fig. 1). The northeast Greenland shelf section consisted of 6 stations covering the Norske-Westwind trough system, 3 stations were sampled in the Norske Trough (17, 18, and 19) and 1 station (11) was sampled in the Westwind Trough (Fig. 1). In addition, 2 more stations (21 and 22) were sampled in front of the largest glacier of northeast Greenland, the 79 N Glacier (Schaffer et al., 2017). Station 21 was located ~20 km away from the glacier front, and station 22 was located in front of the floating glacier ice-tongue.

Immediately after recovery of the CTD rosette, the Go-Flo bottles were carried into a trace metal clean sampling-container where subsampling and filtration was performed under N_2 overpressure (~0.2 Bar) using 0.2 µm filters (Acropack 0.8/0.2 µm cartridge filter, Pall). The samples for dissolved Fe analysis were collected in low density polyethylene bottles (LDPE, 125 mL, Nalgene) immediately acidified to pH 1.8 using ultraclean HCl (Romil Suprapure) on board as described

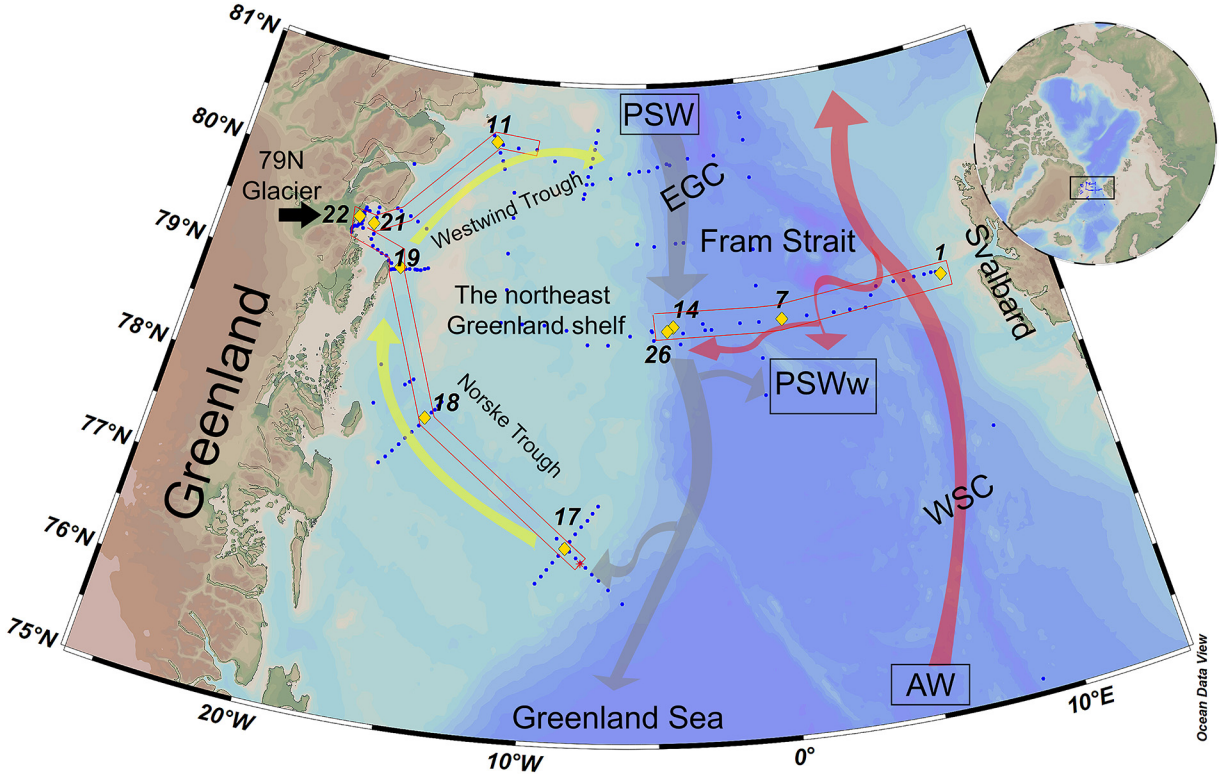

Fig. 1. Map of the study area with schematic currents. The yellow marks indicate the station positions in this study sampled by a trace metal clean CTD Rosette sampling system. The blue dots indicate the stations sampled by a large CTD sampling system. The Fram Strait transect consists of stations 1, 7, 14 and 26. The northeast Greenland shelf transect consist of stations 17, 18 and 19 in the Norske Trough, stations 21 and 22 near the 79 N Glacier terminus, and station 11 in the Westwind Trough. The West-Spitsbergen Current (WSC, indicated by red arrows) brings warm Atlantic Water (AW) into the Arctic Ocean. The southward flowing East Greenland (EGC, grey arrows) carries part of the recirculated WSC as well as outflow Polar Surface Water (PSW) from the Arctic Ocean. The yellow arrows indicate the anti-cyclonic circulation through the trough system. This figure is adapted from Schaffer et al., (2017) and based on Bourke et al., (1987). (For interpretation of the references to colour in this figure legend, the reader is referred to the web version of this article.)

elsewhere (Krisch et al., submitted).

Samples for Fe-binding ligand analysis were collected into acid-cleaned 1000 mL LDPE bottles, immediately stored at −20 °C after sampling, and transported to the NIOZ laboratory for analysis. Prior to analysis, samples were thawed in the dark and sub-samples were taken to determine DFe present in the ligand sample bottles for calculation of total Fe-binding ligand concentrations. Therefore approximately 50 mL was collected into 60 mL pre-cleaned LDPE bottles and acidified to pH ~1.8 using concentrated ultrapure hydrochloric acid into final concentration ~ 0.024 μM (0.2% *v*/v; Seastar chemicals). The acidified samples were stored at room temperature prior to analysis.

2.2. Material handling

Before use, sample bottles were cleaned following three-step cleaning procedure for trace element sample bottles (Cutter, 2010; Middag et al., 2009). All chemicals were prepared using ultrapure water (18.2 MΩ cm, Milli-Q element system, Merck Millipore) and handling performed in an ISO class 7 ultra-clean laboratory with ISO class 5 workspaces. Outside the ultraclean environment, samples were handled in a laminar flood hood (ISO class 5, interflow and AirClean systems).

2.3. Iron analysis

Analysis of DFe was done twice, at GEOMAR, Kiel (Krisch et al., submitted) in samples acidified immediately shipboard, and in sub-samples taken from the ligand samples at NIOZ, Texel. In the laboratory at GEOMAR, DFe concentrations were measured by isotope dilution high-resolution inductively coupled plasma-mass spectrometry (HR-ICP-MS, Thermo Fisher Element XR) after pre-concentration (Rapp et al., 2017). The detailed procedure for DFe determination described elsewhere (Krisch et al., submitted).

For calculation of [L_t] values, we used the DFe measured from the same bottles as the ligand samples. The DFe samples were pre-concentrated using an automated SeaFAST system (SC-4 DX SeaFAST pico; ESI), and analyzed by HR-ICP-MS (Thermo Fisher Element XR) with quantification via standard additions. Accuracy and reproducibility were checked by regular measurements of reference material SAFe D1 (#169) and in-house standards. Results for DFe analyses of reference materials were within the range of May 2013 consensus values (SI Table 1). The average overall method blank (SeaFAST & ICP-MS) concentration, determined by measuring acidified ultrapure water as a sample, was 55 ± 7 pM. Dissolved-Fe concentrations measured from the ligand bottles were approximately 15% (n = 69) lower than DFe measured from immediately acidified samples as also found by Gerringa et al. (2014)

2.4. Fe-binding ligands analysis (TAC Method)

The CLE-AdCSV technique using 2-(2-thiazolylazo)-p-cresol (TAC, Alfa Aesar) was employed to determine the total Fe-binding ligand concentrations, [L_t] and $K'_{Fe'L}$ (Croot and Johansson, 2000).

A Hanging Mercury Drop Electrode stand (VA663 Metrohm), connected to a PC via an interface (IME663) to control the potentiostat (μAutolab III, Metrohm Autolab B.V.) was used. The electrodes in the voltammetric stand included a standard Hg drop working electrode, a glassy carbon counter electrode and a double-junction Ag/AgCl reference electrode (3 M KCl). For the titration, 10 mL subsample aliquots were distributed into the pre-conditioned Teflon (30 mL Savillex) vials, and buffered to a final pH of 8.05 with MnO_2-cleaned borate-

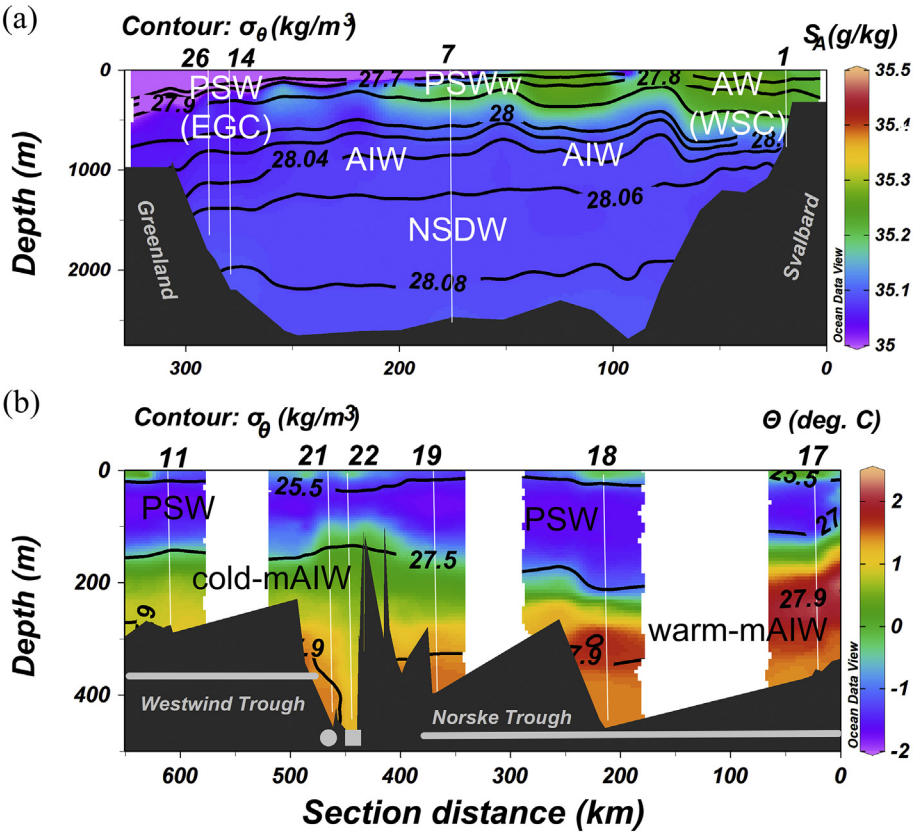

Fig. 2. The distribution of absolute salinity (S_A), conservative temperature (Θ) and potential density (σ_θ) along the transects with the various water masses indicated. (a): Absolute salinity with potential density as contours in the Fram Strait transect; (b): conservative temperature with potential density as contours along the northeast Greenland shelf transect. The square symbol indicates the station (22) in front of the glacier terminus, and the dot symbol indicates the station (21) at ~20 km distance from the glacier terminus.

ammonium (Merck) buffer (final concentration 5 mM). An Fe standard working solution was added to the sample vials, resulting into final concentrations of 0 (twice, no Fe addition); 0.2; 0.4; 0.6; 0.8; 1; 1.2; 1.5; 2; 2.5; 3; 4; 6; 8 (twice) nM of Fe. The purpose of double measurement of the no Fe additions was to be absolutely sure this measurement was not influenced by an unconditioned cell. Based on our experience, a small error of the measurement of the highest addition of the titration has large an effect on the result. Therefore, these points were done twice and the ones that gave the best fit were used for the calculation. After Fe additions, TAC was added to each vial at a final concentration of 10 µM. The content in the vials was allowed to equilibrate for at least 8 h before analysis or typically overnight (Croot and Johansson, 2000). For analysis, the voltammetric scans were in the differential-pulse mode, with a modification from the original procedure (Croot and Johansson, 2000) as previously reported by Slagter et al. (2017). For each sample, two duplicate scans were done at a deposition time of 140 s.

2.5. Fe speciation calculations

The data obtained by CLE-AdCSV was interpreted for the ligand parameters, $[L_t]$ and $K'_{Fe'L}$. The data were fitted by a Langmuir model using non-linear regression using the software package R (R Development Core Team, 2011) as described by (Gerringa et al., 2014). A one-ligand model was applied, assuming a single ligand group existed. This model fitted the data well (SD < 2%; SD of the fitted data from the Langmuir model). The total Fe-binding ligand concentration, $[L_t]$, is reported in nM equivalents of Fe (nM eq. Fe) and $K'_{Fe'L}$ values are reported as a common logarithm to base 10 value (log $K'_{Fe'L}$) with respect to inorganic Fe (Fe′). The prime symbol (′) is used to denote the fraction not bound by L. For the purpose of this paper, we define log $K'_{Fe'L}$ as the binding strength of ligands.

The values of $[L_t]$ and log $K'_{Fe'L}$ were combined with DFe, measured at GEOMAR to derive concentrations of inorganic Fe, [Fe′]. The Fe′ species are predominantly Fe-hydroxides, and at a fixed pH of 8.05, [Fe′] can be calculated (Hudson et al., 1992; Liu and Millero, 2002). The calculation of the ligand parameters is described elsewhere (Gerringa et al., 2014; Ružić, 1982; van den Berg, 1982).

The center of detection window (D) determines which ligand groups, with respect to their conditional binding strength, can be determined. D is defined as the product of the concentration of TAC and the conditional stability constant of $Fe(TAC)_2$, $\beta'_{Fe'(TAC)2}$.

$$D_{TAC} = [TAC]^2 \times \beta'_{Fe'(TAC)2}$$

The inorganic side reaction coefficient of Fe ($\alpha_{Fe'}$) of $10^{10.31}$, as determined using Visual MINTEQ software (Gustafsson, 2011), was used to transform the $\beta'_{Fe'(TAC)2}$ after Croot and Johansson (2000) with respect to Fe^{3+}, into the one with respect to Fe′. Hence, $\beta'_{Fe'(TAC)2} = 10^{12.1}$ was used, resulting in log D_{TAC} = 2.1. The range of the detection window is assumed to be one order above and below log D_{TAC} (Apte et al., 1988).

The side reaction coefficient $\alpha_{Fe'L}$ reflects the ability of ligands to compete for Fe with other ligands and particles. We define $\alpha_{Fe'L}$ here as the competing strength of ligands, expressed as a logarithmic value, log $\alpha_{Fe'L}$. The saturation state of ligands is indicated by the ratio of $[L_t]$/DFe. Assuming that other competing metals can be neglected, ligands are undersaturated when $[L_t]$/DFe > 1, whereas $[L_t]$/DFe ≤1 indicate that the ligands are close to saturation (Thuróczy et al., 2010). Statistical analysis of a *t*-test was performed using the software package R.

3. Results

3.1. Hydrography

The hydrographic features of Fram Strait have been described in detail elsewhere (Beszczynska-Möller et al., 2012; Laukert et al., 2017; Richter et al., 2018; Rudels et al., 2005; Swift and Aagaard, 1981) and are summarized briefly in this study. Water masses were identified

using conservative temperature (Θ in °C) and absolute salinity (S_A in g/kg) plots following definitions by Tomczak and Godfrey (2003). The data of Θ and S_A were derived from the CTD data using Ocean Data View (Schlitzer, 2018).

The relatively warm Atlantic Water (AW) flows northward, carried by the West Spitsbergen Current (WSC) at depths shallower than ~500 m at station 1 (Fig. 2a). In Fram Strait, about half of AW re-circulates back southward, and the other half continues northward into the Arctic Ocean, where it is cooled and freshened, forming Arctic Atlantic Water (AAW) in the process (Bourke et al., 1987; Laukert et al., 2017). The AAW is modified by Pacific-origin water and a large amount of terrestrial runoff in the central Arctic before exiting back through Fram Strait. This modified AAW flows out of the Arctic Ocean along with PSW. These water masses flow southward carried by the East Greenland Current (EGC) (Laukert et al., 2017; Richter et al., 2018; Rudels et al., 2005) in western Fram Strait (at stations 14 and 26; Fig. 2a). The western and middle Fram Strait section is substantially affected by the southward flowing Recirculating-Atlantic Water (RAW). The mixing product of RAW (~200 to ~500 m) and PSW (upper ~300 m), known as warmer PSW (PSWw) (Rudels et al., 2005; Swift and Aagaard, 1981), was observed in surface waters in between the EGC and WSC at station 7 (Fig. 2a). On both sides of Fram Strait, Atlantic Intermediate Water (AIW) (Bourke et al., 1987; Rudels et al., 2005) was present at ~500 to ~900 m depth, and Norwegian Sea Deep Water (NSDW) (Laukert et al., 2017; Swift and Aagaard, 1981) was present below 1000 m. In this study, AIW and NSDW are categorized as deep waters.

Along the northeast Greenland shelf transect, the bathymetry is characterized by the Norske-Westwind Trough system (Fig. 1), that features a deep sill in the Norske Trough and a shallow sill in the Westwind Trough (Schaffer et al., 2017). Along this transect, the surface circulation in the C-shaped trough system carried PSW into the Norske-Westwind Trough system in the upper 150–200 m (Bourke et al., 1987; Schaffer et al., 2017). Underneath the PSW layer, modified-AIW (mAIW) was found deeper than ~200–250 m (Fig. 2b). For the purpose of this study, mAIW is differentiated as warm-mAIW in the Norske Trough and cold-mAIW in the Westwind Trough based on Schaffer et al. (2017).

3.2. Dissolved-Fe and Fe-binding ligands

Here we present DFe profiles (Fig. 3a and b) from stations for which Fe-binding ligand samples were also taken. Higher resolution DFe profiles from GEOTRACES expedition GN05 are reported by Krisch et al., (submitted).

3.2.1. The Fram Strait transect

DFe concentrations in Fram Strait were in the range of 0.28–1.64 nM. Concentrations of DFe in Fram Strait were low in surface waters (median AW = 0.59 nM, PSWw = 0.76 nM, PSW = 0.48 nM) and increased towards the seafloor to 1.28 nM. On the eastern side, a maximum in DFe was present at ~500 m (1.64 nM). This elevated DFe decreased horizontally westward from station 1 in the east to stations 14 and 26 in the west to concentrations of 0.37 nM (Fig. 3a).

In Fram Strait, [L_t] ranged from 0.79 to 3.00 nM eq. Fe (median AW = 1.20 nM eq. Fe, PSWw = 1.77 nM eq. Fe, PSW = 1.78 nM eq. Fe, deep waters = 1.36 nM eq. Fe; SI Table 2). At stations on the western side (14 and 26), [L_t] was generally higher than at stations in the east and central Fram Strait (1 and 7; Fig. 3b). The ratio [L_t]/DFe varied between 0.5 and 5.4 (Fig. 4a). In the central and eastern regions (stations 1 and 7), the ratio decreased below 250 m, whereas it remained high on the western side of Fram Strait (stations 14 and 26). The ligands were saturated with Fe ([L_t]/DFe < 1) at 500 m depth at station 1 and nearly saturated near the sea floor.

Whilst [L_t] in surface waters of Fram Strait generally increased from AW (median = 1.20 nM eq. Fe) in the east to PSW (median = 1.77 nM eq. Fe) in the west (Figs. 3b and 5a), the median of [Fe′] in Fram Strait was relatively uniform at 0.05–0.15 pM (Fig. 5b), apart from the two samples where organic ligands were saturated with Fe.

A considerable variation was observed in log $K'_{Fe'L}$ values (Fig. 6a) that ranged from 11.8 to 13.9 (median AW = 13.3, PSWw = 12.9, PSW = 12.4, deep waters = 13.0; Fig. 6a). The values of log $\alpha_{Fe'L}$ (Fig. 6b) varied between 1.3 and 4.7 (median AW = 4.0, PSWw = 3.7, PSW = 3.4, deep waters = 3.9; Fig. 6b). The highest log $\alpha_{Fe'L}$ value falls more than 2 orders of magnitude above the log D_{TAC} and thus the highest log $K'_{Fe'L}$ could not be estimated accurately. Since the ligands were saturated with DFe at 500 m depth at station 1, the calculated $\alpha_{Fe'L}$ does not represent the actual value of ligand competing strength and

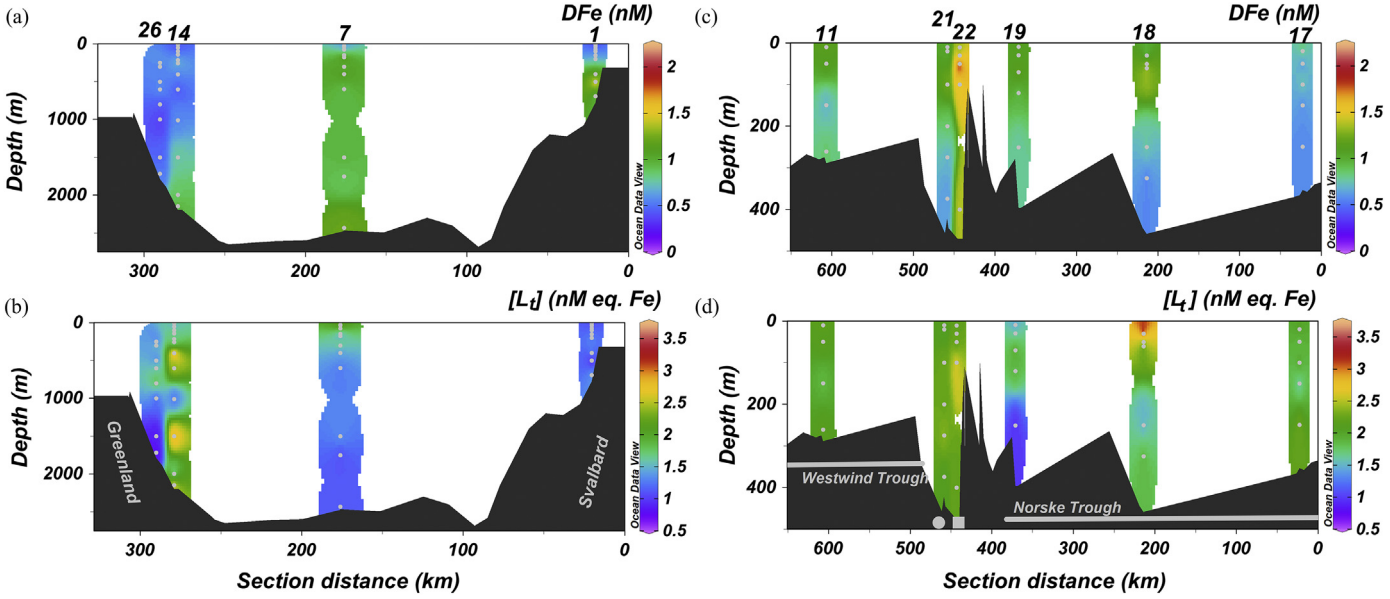

Fig. 3. The distribution of dissolved Fe (DFe, data from Krisch et al., submitted) and total Fe-binding ligand concentrations ([L_t]) of both transects; the Fram Strait transect on the left and the northeast Greenland shelf transect on the right. DFe concentrations (a,c) and [L_t] (b,d). Along the northeast Greenland shelf transect, the square symbol indicates the station in front of the glacier terminus, and the dot symbol indicates the station at ~20 km distance from the glacier terminus.

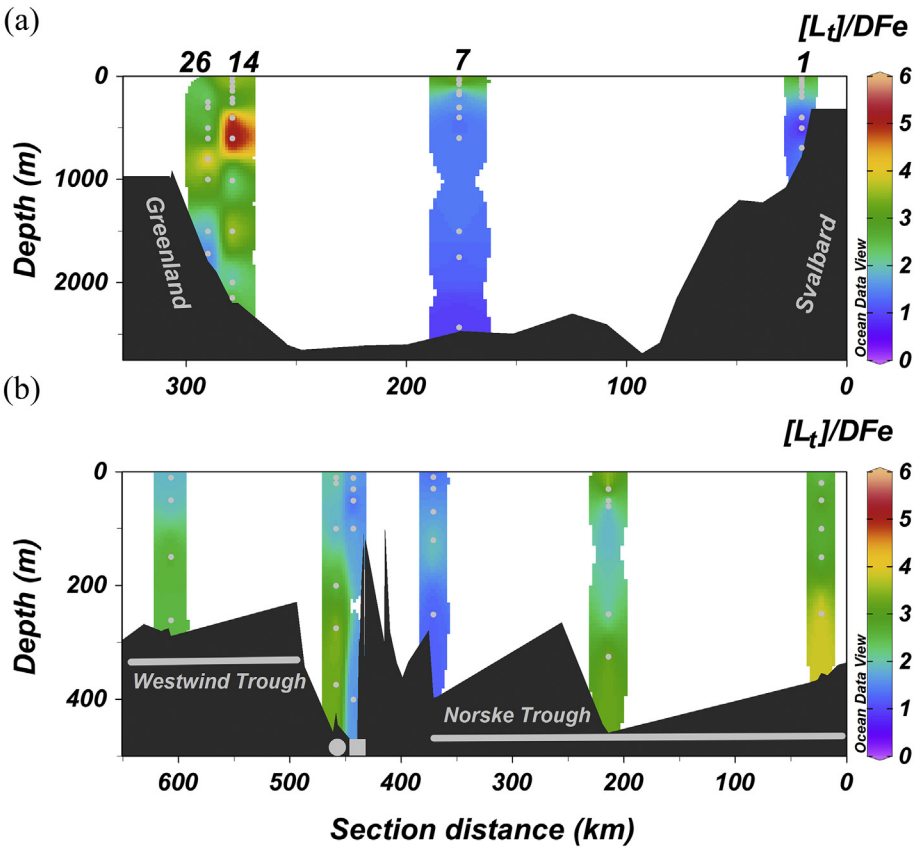

Fig. 4. The distribution of ligand saturation ([L_t]/DFe) of both transects; the Fram Strait transect (a) and the northeast Greenland shelf transect (b). Along the northeast Greenland shelf transect, the square symbol indicates the station in front of the glacier terminus, and the dot symbol indicates the station at ~20 km distance from the glacier terminus.

thus this data point was not used for calculations.

3.2.2. The northeast Greenland shelf transect

Concentrations of DFe ranged from 0.58 to 1.45 nM in PSW (median DFe = 0.92 nM) and 0.55 to 0.78 nM in warm-mAIW (median DFe = 0.68 nM) in the Norske Trough (Fig. 3c). Near the 79 N Glacier terminus and Westwind Trough, DFe concentrations ranged from 0.71 to 2.10 nM (median DFe = 1.16 nM) in PSW and 0.63 to 1.38 nM in cold-mAIW (median DFe = 0.77 nM). The highest DFe concentration (2.10 nM) was found in PSW at 30 m depth in front of the glacier terminus (station 22).

In the Norske Trough, [L_t] varied from 1.41 to 3.60 nM eq. Fe in PSW and 0.97 to 2.26 nM eq. Fe in warm-mAIW, whereas near the glacier terminus and Westwind Trough, [L_t] ranged from 1.88 to

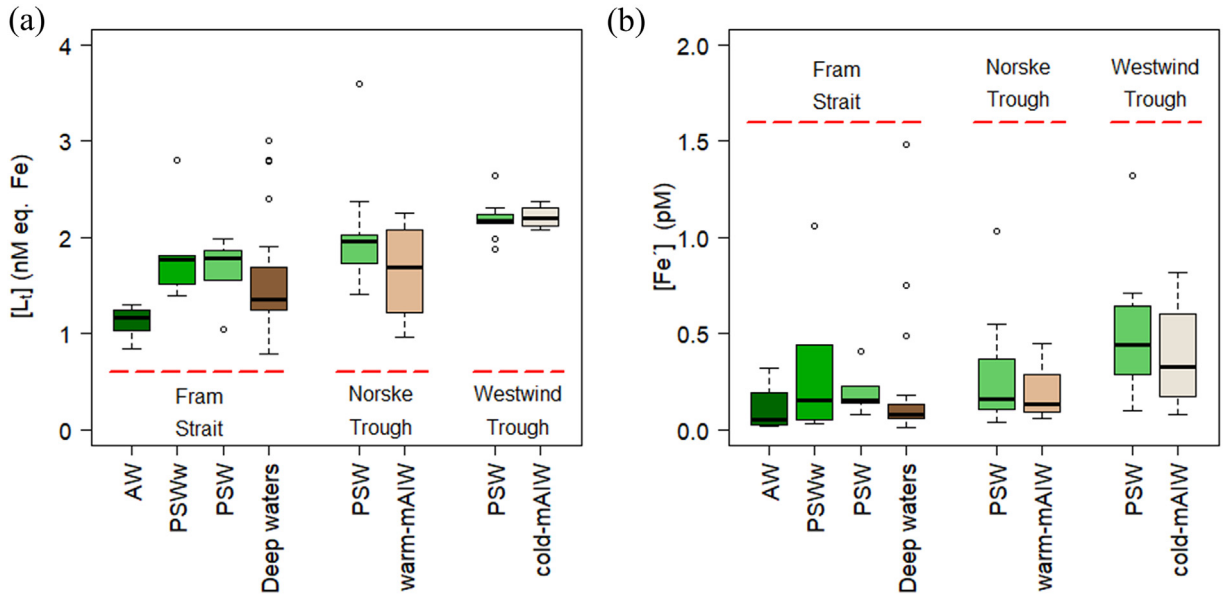

Fig. 5. Boxplots of the concentrations of (a) total organic Fe-binding ligands, [L_t], and (b) inorganic iron, [Fe´], from all stations in Fram Strait and over the northeast Greenland shelf (the Norske Trough and Westwind Trough), categorized by water mass. Indicated are the median value by a thick horizontal line, the box contains the first and third quartiles, the whiskers are the range of data excluding the outliers. The circles indicate the outliers being 1.5* interquartile range from the box (Teetor, 2011).

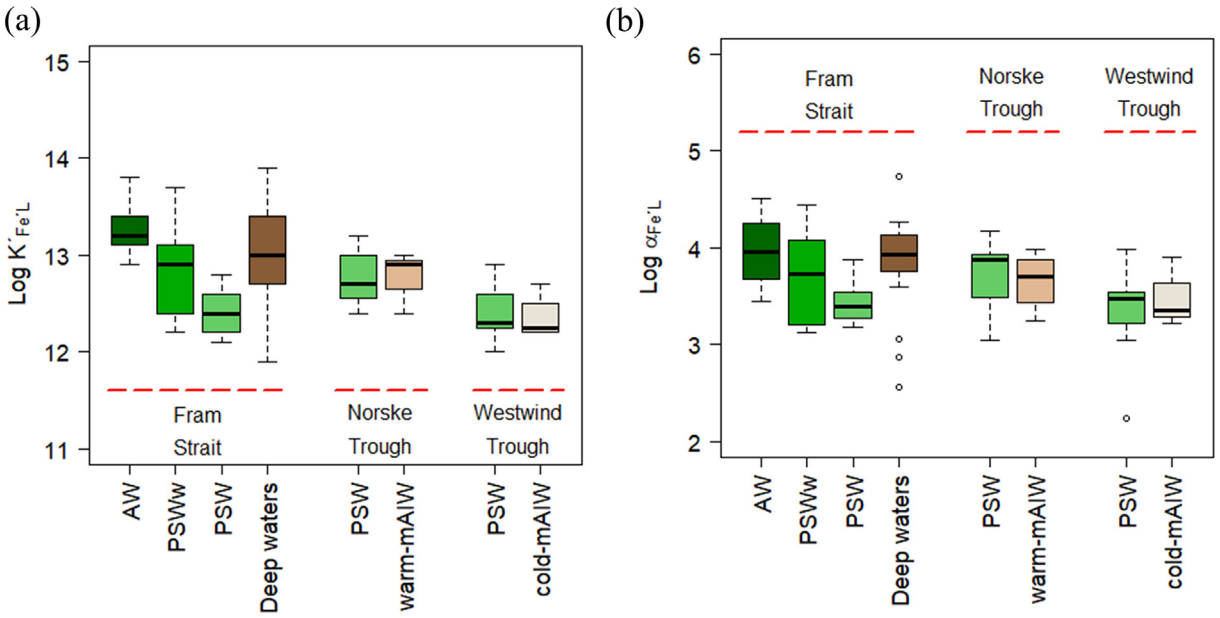

Fig. 6. Boxplots of the conditional stability constants (binding strength), log $K'_{Fe'L}$ (a) and side reaction coefficients (competing strength), log $\alpha_{Fe'L}$ (b) from all stations in Fram Strait and over the northeast Greenland shelf (the Norske Trough and Westwind Trough), categorized by water mass. The detail explanation of the boxplot is as described in Fig. 5.

2.64 nM eq. Fe in PSW and 2.08 to 2.38 in cold-mAIW (Fig. 3d, SI Table 2). On average, [L_t] was slightly higher at stations near the glacier terminus (stations 21 and 22) than in the Norske Trough, although the highest [L_t] existed in PSW in the Norske Through (station 18) with values up to 3.60 nM eq. Fe at 30 m depth. The ratio of [L_t]/DFe ranged between 1 and 4.4 (Fig. 4b), indicating that Fe-binding ligands along the northeast Greenland shelf transect were undersaturated. Near the seafloor at station 19 (Norske Through) and at 50 m depth at station 22 (glacier terminus), nearly saturated ligands were observed.

Generally, organic ligands were present at higher concentrations in PSW and mAIW near the glacier terminus and Westwind Trough than in the Norske Trough and Fram Strait (Fig. 5a). High concentrations of [Fe´] were found in PSW and cold-mAIW in front of the floating glacier ice-tongue (Fig. 5b), where the organic ligands were nearly saturated (at station 22; Fig. 4b). Excluding high [Fe´] concentrations in samples where organic ligands were nearly saturated, the median of [Fe´] in PSW and mAIW was lower in the Norske Trough (0.16 and 0.13 pM) than the Westwind Trough and near the glacier terminus (0.41 and 0.33 pM) (Fig. 5b).

The log $K'_{Fe'L}$ ranged from 12.4–13.2 in the Norske Trough (median PSW = 12.7, warm-mAIW = 12.9; Fig. 6a). Near the glacier terminus and in the Westwind Trough, the log $K'_{Fe'L}$ ranged from 12.0–12.9 (median PSW and cold-mAIW = 12.3, warm-mAIW = 12.9; Fig. 6a). The log $K'_{Fe'L}$ in the northeast Greenland shelf waters were on average lower than in Fram Strait (Fig. 6a). The median values of log $\alpha_{Fe'L}$ in PSW and warm-mAIW in the Norske Trough were 3.9 and 3.7, respectively. In the Westwind Trough and in front of glacier terminus, the median values of log $\alpha_{Fe'L}$ were 3.5 in PSW and 3.4 in cold-mAIW. In general, variation in log $\alpha_{Fe'L}$ values over the northeast Greenland shelf was less than in Fram Strait (Fig. 6b).

4. Discussion

The applied method using TAC was reported to underestimate [L_t] due to an interaction of TAC with HS binding sites (Laglera et al., 2011; Slagter et al., 2019). However, this method did reveal HS involvement in the ligand pool in different environments (Batchelli et al., 2010; Dulaquais et al., 2018), even in the TPD flow path, where the HS ligands were the dominant group (Slagter et al., 2017). Slagter et al. (2019) compared two CLE-AdCSV techniques, TAC and salicylaldoxime (SA) in the Arctic Ocean and concluded that an offset in [L_t] between the methods existed. Yet, the increase in [L_t] due to HS ligands in the TPD was the same for both methods. Thus in our study, we assume that HS is detectable by the TAC method, although [L_t] might be underestimated.

4.1. Comparison to previous studies

Natural ligand measurements have not previously been reported for Fram Strait, but data is available for adjacent areas, notably the Northern Atlantic (Buck et al., 2015; Gerringa et al., 2015; Mohamed et al., 2011) and Arctic Ocean (Slagter et al., 2017; Thuróczy et al., 2011). The studies conducted by Thuróczy et al. (2011), Gerringa et al. (2015) and Slagter et al. (2017) used the same analytical method and data processing technique as in this study, allowing a direct comparison. The here reported [L_t] in Fram Strait (median PSW = 1.78 nM eq. Fe, PSWw = 1.77 nM eq. Fe, SI Table 2) is comparable to the median [L_t] (1.61 nM eq. Fe) outside the TPD flow path (Slagter et al., 2017), but slightly higher than [L_t] reported by Gerringa et al. (2015) for the region between 60 and 33°N in the north west Atlantic Ocean where the median [L_t] was 1.2 nM eq. Fe (N = 8) and reached up to 3.3 nM eq. Fe (SI Fig. 2). The median [L_t] in PSW in the western Fram Strait (1.78 nM eq. Fe) and in the northeast Greenland shelf waters (1.96 and 2.17 nM eq. Fe, SI Table 2; surface shelf waters = 2.06 nM eq. Fe; SI Fig. 2) was comparable to the median [L_t] (2.02 nM eq. Fe) reported by Thuróczy et al. (2011) for the Arctic Ocean, but lower than the average [L_t] (2.79 ± 0.92, N = 19) inside the TPD flow path (Slagter et al., 2017). The elevated [L_t] in the TPD has been related to HS ligands from fluvial input as well as interaction between sea-ice and sediment (Slagter et al., 2017 and references therein). Gerringa et al. (2015) hypothesized that the Arctic is a source of ligands, largely of humic origin, to the North Atlantic and that [L_t] decreases over time and distance during advection to the south with North Atlantic Deep Water. The current data in Fram Strait indeed confirmed the Arctic can be a source of ligands, likely of humic origin, to regions to the south.

We found high [L_t] up to 3.6 nM eq. Fe in the sea-ice covered PSW in the Norske Trough (station 18). Antarctic sea ice is known to be a source of ligands, probably due to EPS excretion at the bottom of the

sea ice by diatoms. According to Lannuzel et al. (2015), abundant sea ice diatoms were responsible for relatively high [L_t] in under-ice seawater (4.9 to 9.6 nM eq. Fe; log $K'_{Fe'L}$ ~11 to 13 measured with 1-nitroso-2-napthol), indicating that EPS could increase [L_t] in seawater with sea-ice coverage. As far as we know, no ligand data of Arctic sea ice is available, but the high [L_t] in the sea-ice covered in the Norske Trough, was only slightly lower than the [L_t] reported by Lannuzel et al. (2015) and had comparable relatively high log $K'_{Fe'L}$ (12.4–12.8). As detailed in the introduction, EPS were considered to be part of the weak ligand group (Buck et al., 2016; Bundy et al., 2014; Hassler et al., 2011; Hassler et al., 2017; Laglera and van den Berg, 2009), but Norman et al. (2015) demonstrated that EPS could have strong conditional stability constants (log $K'_{Fe'L} > 12$), hence could contribute to the strong ligands detected in surface waters, especially in regions with sea-ice coverage (Krembs et al., 2002; Lannuzel et al., 2015; Lin and Twining, 2012). Thus we suggest that the high [L_t] in sea-ice covered Norske Trough is possibly due to EPS.

4.2. Organic ligand sources in Fram Strait

A considerable variation in log $K'_{Fe'L}$ values (median AW = 13.3, PSWw = 12.9, PSW = 12.4; Fig. 6a), suggests varying contributions of relatively strong and weak ligand groups to the overall ligand pool. The Fe-binding ligands in surface waters of Fram Strait were dominated by a strong ligand group as apparent from the relatively high log $K'_{Fe'L}$(> 12; Fig. 6a). Despite seasonal NO_3 depletion (Hopwood et al., 2018), this area is productive (Cherkasheva et al., 2014; Smith Jr. et al., 1987). Primary productivity is a known source of organic ligands in surface waters as high ligand concentrations are often associated with high chlorophyll-*a* concentrations (Boye et al., 2001; Gledhill and Buck, 2012; Hunter and Boyd, 2007; Rue and Bruland, 1995; van den Berg, 1995). Besides releasing EPS, marine bacteria (*Alteromonas sp.*) can also synthesize siderophores during a bloom (Hogle et al., 2016). Additionally, following the decline of a phytoplankton bloom, excessive production of EPS can occur (Decho and Gutierrez, 2017). A high weekly average of chlorophyll-*a* concentrations was observed using the MODIS satellite (https://giovanni.gsfc.nasa.gov/giovanni/), which indicates the presence of a phytoplankton bloom in June and July. Our sampling time in Fram Strait (end of July to early August 2016) coincided with the post-bloom period and therefore it seems likely that bloom-associated ligands are responsible for the relatively high concentration of strong ligands in surface waters of Fram Strait.

The surface ligand concentration (Fig. 5a) on the western side of Fram strait (median PSW = 1.78 nM eq. Fe) as well as further into central Fram Strait (median PSWw = 1.77 nM eq. Fe) was somewhat higher than in eastern Fram Strait (median AW = 1.20 nM eq. Fe). Lateral transport of TPD-carried HS ligands from the Arctic (Laglera et al., 2019a; Slagter et al., 2019), likely formed an additional ligand source to surface waters of the western Fram Strait, where PSW flows south with the EGC in the upper ~150 m (Laukert et al., 2017; Richter et al., 2018). This implies both the phytoplankton bloom and TPD may play a role in the surface composition and distribution of ligands in Fram Strait. Atmospheric input does not seem to influence ligand concentrations, Rijkenberg et al. (2008) and Wagener et al. (2008) have shown that there is no input of aeolian Fe-binding ligands during dust deposition events, but dissolution of Fe from the dust does depend on the Fe-binding ligands present in seawater.

The organic ligands in Fram Strait were almost saturated near the seafloor (Fig. 4a), notably in the region with elevated DFe concentrations (station 7). The western Fram Strait (stations 14 and 26) had relatively high, but variably distributed [L_t] over the water column (Fig. 3b, SI Fig. 1). Slope sediments can serve as a source of ligands to the deeper part of the water column (Buck and Bruland, 2007), however this does not seem to be the case for the station nearest to the slope (station 26), in contrast to the station further into Fram Strait (station 14). Possibly the water transport along the shelf break and interaction with the slope is not constant with time and place. Eddies exist at the shelf break and can reach deep enough to propagate subsurface waters (i.e AIW) towards the inner shelf (Schaffer et al., 2017; Topp and Johnson, 1997). In addition, here at this latitude (79°N) the core of the southward flowing RAW mixes with the PSW, and thus substantially contribute to the EGC (Richter et al., 2018). Water transport driven by eddies and RAW intrusion to the EGC may explain the variably distributed [L_t] in the upper (~500 m) water column, however, the elevated concentrations in the deeper part of station 14 remain unexplained.

4.3. Organic ligand sources over the northeast Greenland shelf

In this section, the transect over the northeast Greenland shelf will be discussed in the direction of the general circulation, starting at the southern inlet and going along the Norske Trough towards the 79 N Glacier and back towards Fram Strait via the Westwind Trough. The water masses from Fram Strait are propagated towards the inner shelf at the southern inlet (station 17), potentially by eddies, while undergoing pronounced mixing at the shelf edge. Eddy stirring and tidal mixing seem to be persistent features in the Norske Trough inlet (Bourke et al., 1987; Budéus et al., 1997; Schaffer et al., 2017). The balance between release and removal of organic ligands, along with physical water mass mixing (Budéus et al., 1997), is likely responsible for the fairly constant [L_t] observed in the water column at station 17 (Fig. 3d).

The relatively high concentrations of strong organic ligands (up to 3.60 nM eq. Fe, log $K'_{Fe'L}$ 12.4–12.8) observed in PSW in the Norske Trough were most likely related to an earlier bloom, generating marine HS and EPS ligand groups with relatively strong affinity for Fe. The macro-nutrients (NO_3, PO_4, Si; data not shown) at this location were depleted and DFe was low (Fig. 3d), indicative of a prior bloom. Consistently the chlorophyll-*a* concentration was low at the time of sampling (unpublished data), whereas higher concentrations were observed via satellite in the period prior to sampling (https://giovanni.gsfc.nasa.gov/giovanni/). Sato et al. (2007) showed a relation between increasing [L_t] and decreasing chlorophyll-*a* due to zooplankton grazing, and Laglera et al. (2019b) measured an increase in strong organic ligands as a consequence of grazing. This demonstrated that declining blooms can indeed contribute strong organic ligands and increase [L_t] as we observed in our study region. Additionally, black sea-ice with entrapped sediment was spotted during sampling at this location and the melting of black sea-ice can release HS ligands (Genovese et al., 2018) in addition to ligands released from grazing (Decho and Gutierrez, 2017; Laglera et al., 2019b). Also, we cannot eliminate the possible contribution of EPS, either produced in situ by sea-ice diatoms (Lannuzel et al., 2015) or released by phytoplankton cells after bloom termination (Decho and Gutierrez, 2017). Recent studies pointed out that HS and EPS can have strong Fe-binding sites (Laglera et al., 2019b; Lannuzel et al., 2015; Norman et al., 2015; Slagter et al., 2019). Therefore, the presence of HS and EPS can contribute to the pool of relatively strong ligands with elevated [L_t] in PSW in the Norske Trough.

The ligand-rich PSW in the Norske Trough did not seem to be a significant contributor of organic ligands to either the glacier front or the glacier outflow. Probably ligands produced in the Norske Trough did not yet reach the glacier front. In addition, newly produced ligands associated with primary productivity over the shelf, such as at station 18, are likely to be partially lost due to photodegradation (Barbeau et al., 2001; Powell and Wilson-Finelli, 2003), aggregation and sinking (Cullen et al., 2006) during transport. Either way, a high ligand concentration, such as in the surface waters of Norske Trough, was not observed at the glacier terminus (at stations 21 and 22). At the 79 N Glacier terminus, the 80–120 m thick ice-front is limiting direct entry of PSW into the glacier cavity, and at depths of ~80–270 m, water flows eastward away from the glacier front and into the trough system (Schaffer et al., 2017). As warm-mAIW in the Norske Trough has a

relatively low [L_t], notably at station 19 on the northern end of the Norske Trough, ligands in the glacier outflow are thus likely produced in the glacier cavity itself. In general, meltwater is relatively poor in DOC compared to coastal seawater, but this DOC may be highly available to bacteria (Paulsen et al., 2017). Hence, the relatively high [L_t] over the entire water column near the 79 N Glacier terminus (Fig. 3d), could be associated with bacterial remineralization or by-products of organic matter degradation (Gledhill and Buck, 2012; Gordienko and Laktionov, 1969; Hunter and Boyd, 2007). These ligands would be transported into the Westwind Trough, following the anti-cyclonic water circulation of the Norske-Westwind Trough system (Schaffer et al., 2017; Topp and Johnson, 1997). The median of log $K'_{Fe'L}$, both in the PSW and mAIW near the glacier terminus (stations 21 and 22) and Westwind Trough (station 11) were somewhat lower (Fig. 6a) than in the Norske Trough (median log $K'_{Fe'L}$ =12.3 versus 12.7 and 12.9). This indicates that different ligand sources shift the characteristics of the overall ligand pool or the ligand pool has undergone physical, chemical or biologically-induced structural alterations during transport, e.g. through photo- or microbial degradation. Although ligands were present at higher concentrations (Figs. 3d and 5a), these organic ligands were weaker than in the Norske Trough (Fig. 6a). Primary productivity likely dominated the organic ligand sources in the Norske Trough, which may have led to a ligand pool with a relatively high conditional stability constant. In contrast, near the glacier terminus and in Westwind Trough, bacterial remineralization most likely was the dominant ligand source, resulting in more, but overall weaker ligands.

Near the glacier terminus and in Westwind Trough, [Fe´] was relatively high compared to Norske Trough and Fram Strait (Fig. 5b). The glacier acts as a source of Fe and organic-ligand bound Fe, thereby facilitating glacial-Fe transport. However, at the glacier terminus, Fe was prone to precipitation and/or scavenging as [Fe´] was enhanced (Fig. 5b) and the competing strength of the ligands (log $\alpha_{Fe'L}$) was relatively low (Fig. 6b). It should be noted here that the complexation of Fe by organic ligands is an equilibrium reaction between complexed Fe and [Fe´], where [Fe´] is not only determined by competing strength, but also by the scavenging intensity and precipitation reactions. Thus the ligands can effectively release Fe if their competing strength is relatively low and they are outcompeted by scavenging and precipitation processes as shown in the deep Makarov Basin (Slagter et al., 2017; Thuróczy et al., 2011). Availability of [L_t] is thus not a guarantee for complexing (additional) DFe, as it is the overall equilibration between excess ligands, scavenging sites and precipitation that governs the fate of DFe.

4.4. Biogeochemical provinces of organic ligands

This study distinguished three biogeochemical provinces with respect to Fe-binding ligands, based on the influence of different sources of ligands, and hence ligand properties and distribution. The biogeochemical provinces include (1) Fram Strait, (2) Norske Trough and (3) near the glacier terminus and Westwind Trough. The different ligand properties and distribution are reflected in the differences in [L_t] (Fig. 5a), log $K'_{Fe'L}$ (Fig. 6a) and log $\alpha_{Fe'L}$ (Fig. 6b).

As described above, in the northward flowing AW of the eastern Fram Strait, strong organic ligands derived from phytoplankton blooms are suggested to dominate the ligand pool. Whereas in the western Fram Strait in southward flowing PSW, part of the ligands probably originated from the Arctic Ocean and partly consists of HS ligands carried by the TPD (Slagter et al., 2017). The average log $K'_{Fe'L}$ is significantly higher (SI Table 3) in the AW flow (mean log $K'_{Fe'L}$ = 13.3 ± 0.3 (1 SD); SI Table 2), compared to the PSW flow in western Fram Strait where the influence of Arctic waters resulted in lower log $K'_{Fe'L}$ values (the mean of log $K'_{Fe'L}$ 12.4 ± 0.3 (1 SD); SI Table 2). The range in log $K'_{Fe'L}$ is relatively broad (Fig. 6a), implying that different ligand sources supply ligands with various chemical properties, thus different affinity to bind Fe.

As detailed, organic ligands were present at higher concentrations near the glacier terminus and Westwind Trough than in the Norske Trough and Fram Strait (Figs. 3b and 5a), but the ligands near the glacier terminus and Westwind Trough had a lower affinity for binding Fe (Fig. 6a) and a lower competing strength, log $\alpha_{Fe'L}$ (Fig. 6b). Krisch et al., (submitted) observed that glacial-derived Fe transfer through the Westwind Trough was low because of a net transfer of Fe from the colloidal (thus part of DFe) to the particulate phase with subsequent settling out of the water column, an important removal process in the Fe cycle (Wu et al., 2001). Although organic ligands exist in both the soluble and colloidal fractions (Boye et al., 2010; Fitzsimmons et al., 2015; Thuróczy et al., 2011), part of the colloidal Fe fraction is inert, and not exchangeable (Cullen et al., 2006) and might contribute to coagulation and aggregation and disappearance of Fe. We did not separate soluble and colloidal fractions, but we do demonstrate that the ligands in the glacier outflow and Westwind Trough were relatively weak with a lower competing strength (Fig. 6a and b). This results in a relatively high [Fe´] which in turn allow loss of DFe via precipitation and/or scavenging, consistent with the loss of colloidal Fe observed by Krisch et al., (submitted).

Global warming causes rapid environmental changes in the Arctic and sub-Arctic Oceans (Gascard et al., 2008; IPCC, 2014) to which Fram Strait belong (Ekwurzel et al., 2001; Schuur et al., 2015). These changes may alter the properties and distribution of organic Fe-binding ligands. Melting of sea-ice influences biological activity (Arrigo et al., 2008; Meier et al., 2014) and without considering possible nutrient depletion, this may increase the release of strong organic ligands. An increased competing strength of organic ligands enhances the ability of ligands to stabilize additional Fe input, potentially increasing the DFe export from Greenland towards the open ocean if the timing and location of DFe input coincides with the presence of these ligands. Not much is known about Fe limitation in the Nordic Seas, although potential Fe limitation was reported for the Nansen Basin of the Arctic Ocean (Rijkenberg et al., 2018). Also the Iceland Basin in the North Atlantic experiences seasonal Fe limitation (Hopwood et al., 2018; Mohamed et al., 2011; Nielsdóttir et al., 2009; Ryan-Keogh et al., 2013). Enhanced transport of ligand bound Fe from the Arctic may thus have a profound effect on primary productivity in the high-latitude North Atlantic. However, such changes must also be considered alongside other physical/chemical perturbations in the region as a result of ongoing changes such as the increase in freshwater discharge around Greenland. The complex interplay between Fe and ligand sources versus scavenging and coagulation will need to be better constrained to enable accurate predictions of changes in the biogeochemical cycle of Fe in the globally important northern high latitudes, as well as elsewhere.

5. Conclusions

This study provides a connection between the previous reports on organic Fe-binding ligands in the Arctic Ocean and North Atlantic Ocean, as well as insight into the competing strength of organic Fe-binding ligands that regulate DFe transport from a Greenland glacier. Our results indicate that the Fe-binding ligands in surface waters of Fram Strait originate from microbial activity with addition from southward-flowing TPD transported terrestrial ligands on the western side of Fram Strait. Given that the [L_t] in western Fram Strait is intermediate to the higher concentrations reported for the Arctic and the lower concentrations reported for the North Atlantic, this confirms the decreasing [L_t] southward from the Arctic Ocean.

In the Norske Trough, the remnant from an earlier bloom was likely the main source of organic Fe-binding ligands in surface waters, as the contribution of ligands can be substantial at the base of sea-ice. The elevated [L_t] at stations near the 79 N Glacier terminus is probably associated with remineralization of glacially-derived organic matter. Our data shows that even though significantly higher concentrations of

organic ligands were present at the vicinity of 79 N Glacier terminus and in the Westwind Trough (outflow) than in the Norske Trough (inflow), the organic ligands are weaker and therefore can compete less efficiently with scavenging processes and precipitation. Especially close to the glacier, ligands have a weaker affinity for binding Fe. We show that transport of Fe in the glacial outflow is potentially regulated by ligands as has been anticipated from comparisons of particulate and dissolved Fe distributions in several systems worldwide. Additionally, our results reveal the underlying mechanism where the lower ligand binding strength and consequently higher [Fe′] (rather than a low concentration of ligands) result in more precipitation of Fe-oxyhydroxides or/and scavenging. Thereby only a small part of the glacial DFe will be transported over the shelf into the ocean. Different sources supply ligands with various chemical properties, resulting in distinctive properties of the ligand pool among regions.

Rapid environmental changes due to global warming will cause increased river runoff and glacial melt into the Arctic Ocean, increasing gross Fe supply into the Arctic basin. However, it is the combination of availability and binding strength of organic ligands that regulate DFe transport and distribution in Fram Strait region. Thus, to understand the consequences of global warming in the Arctic and sub-Arctic Oceans for the biogeochemical cycle of Fe, the changes in the biogeochemical cycle of the ligands need to be understood as well. Especially glacial systems will need to be investigated further to determine if there is strong temporal variability in the concentration and competing strength of Fe-binding ligands or if large differences exist between different glaciers.

Supplementary data to this article can be found online at https://doi.org/10.1016/j.marchem.2020.103815.

Acknowledgements

Authors would like to thanks Captain Schwarze and his crew of the RV Polarstern, as well as chief scientist Torsten Kanzow, for their effort and support during sample collection. Patrick Laan is acknowledged for analyzing DFe for Fe-binding ligands calculation. We thank anonymous reviewers for their comments that improved the manuscript considerably. IA was financed by Indonesia Endowment Fund for Education (LPDP), and SK was financed by GEOMAR and the German Research Foundation (DFG award number AC 217/1-1 to E. P. A). Figs. 1 to 4 are made using the software Ocean Data View 5.1.7 (Schlitzer, 2018). Figures 5 and 6 are made using the software package R version 3.4.2. Data can be found online at https://doi.org/10.25850/nioz/7b.b.u.

References

Abualhaija, M.M., van den Berg, C.M.G., 2014. Chemical speciation of iron in seawater using catalytic cathodic stripping voltammetry with ligand competition against salicylaldoxime. Mar. Chem. 164, 60–74.
Apte, S.C., Gardner, M.J., Ravenscroft, J.E., 1988. An evaluation of voltammetric titration procedures for the determination of trace metal complexation in natural waters by use of computers simulation. Anal. Chim. Acta 212, 1–21.
Arrigo, K.R., van Dijken, G., Pabi, S., 2008. Impact of a shrinking Arctic ice cover on marine primary production. Geophys. Res. Lett. 35 (19).
Barbeau, K., Rue, E.L., Bruland, K.W., Butler, A., 2001. Photochemical cycling of iron in the surface ocean mediated by microbial iron(iii)-binding ligands. Nature 413 (6854), 409–413.
Batchelli, S., Muller, F.L.L., Chang, K.-C., Lee, C.-L., 2010. Evidence for strong but dynamic Iron − humic colloidal associations in humic-rich coastal waters. Environ. Sci. Technol. 44 (22), 8485–8490.
Beszczynska-Möller, A., Fahrbach, E., Schauer, U., Hansen, E., 2012. Variability in Atlantic water temperature and transport at the entrance to the Arctic Ocean, 1997–2010. ICES J. Mar. Sci. 69 (5), 852–863.
Bourke, R.H., Newton, J.L., Paquette, R.G., Tunnicliffe, M.D., 1987. Circulation and water masses of the East Greenland shelf. J. Geophys. Res. 92 (C7), 6729–6740.
Boyd, P.W., et al., 2000. A mesoscale phytoplankton bloom in the polar Southern Ocean stimulated by iron fertilization. Nature 407, 695.
Boye, M., et al., 2001. Organic complexation of iron in the Southern Ocean. Deep-Sea Res. 48 (6), 1477–1497.
Boye, M., et al., 2010. Significant portion of dissolved organic Fe complexes in fact is Fe colloids. Mar. Chem. 122 (1), 20–27.
Buck, K.N., Bruland, K.W., 2007. The physicochemical speciation of dissolved iron in the Bering Sea, Alaska. Limnol. Oceanogr. 52 (5), 1800–1808.
Buck, K.N., Sohst, B., Sedwick, P.N., 2015. The organic complexation of dissolved iron along the U.S. GEOTRACES (GA03) North Atlantic Section. Deep-Sea Res. II Top. Stud. Oceanogr. 116, 152–165.
Buck, K.N., Gerringa, L.J.A., Rijkenberg, M.J.A., 2016. An Intercomparison of dissolved Iron speciation at the Bermuda Atlantic time-series study (BATS) site: results from GEOTRACES Crossover Station A. Front. Mar. Sci. 3 (262).
Budéus, G., Schneider, W., Kattner, G., 1997. Distribution and exchange of water masses in the Northeast Water polynya (Greenland Sea). J. Mar. Syst. 10 (1), 123–138.
Bundy, R.M., Biller, D.V., Buck, K.N., Bruland, K.W., Barbeau, K.A., 2014. Distinct pools of dissolved iron-binding ligands in the surface and benthic boundary layer of the California Current. Limnol. Oceanogr. 59 (3), 769–787.
Burkhardt, B.G., Watkins-Brandt, K.S., Defforey, D., Paytan, A., White, A.E., 2014. Remineralization of phytoplankton-derived organic matter by natural populations of heterotrophic bacteria. Mar. Chem. 163, 1–9.
Calace, N., et al., 2001. Aquatic humic substances in pack ice-seawater-sediment system. Int. J. Environ. Anal. Chem. 79 (4), 315–329.
Cherkasheva, A., et al., 2014. Influence of the physical environment on polar phytoplankton blooms: a case study in the Fram Strait. J. Mar. Syst. 132, 196–207.
Croot, P.L., Johansson, M., 2000. Determination of Iron speciation by Cathodic stripping voltammetry in seawater using the competing ligand 2-(2-Thiazolylazo)-p-cresol (TAC). Electroanalysis 12 (8), 565–576.
Cullen, J.T., Bergquist, B.A., Moffett, J.W., 2006. Thermodynamic characterization of the partitioning of iron between soluble and colloidal species in the Atlantic Ocean. Mar. Chem. 98 (2), 295–303.
Cutter, G., Andersson, P., Codispoti, L., Croot, P., François, R., Lohan, M.C., Obata, H., Rutgers, V.D., Loeff, M., 2010. Sampling and Sample-handling Protocols for GEOTRACES Cruises.
De Baar, H.J.W., 1990. On iron limitation of the Southern Ocean : experimental observations in the Weddell and Scotia Seas. Marine Ecol. Prog. Ser. 65, 105–122.
Decho, A.W., Gutierrez, T., 2017. Microbial extracellular polymeric substances (EPSs) in ocean systems. Front. Microbiol. 8 (922).
R Development Core Team, 2011. R: A Language and Environment for Statistical Computing. R foundation for statistical computing, Vienna, Austria.
Dulaquais, G., et al., 2018. The biogeochemistry of electroactive humic substances and its connection to iron chemistry in the North East Atlantic and the Western Mediterranean Sea. J. Geophys. Res. 123 (8), 5481–5499.
Ekwurzel, B., Schlosser, P., Mortlock, R.A., Fairbanks, R.G., Swift, J.H., 2001. River runoff, sea ice meltwater, and Pacific water distribution and mean residence times in the Arctic Ocean. J. Geophys. Res. 106 (C5), 9075–9092.
Fitzsimmons, J.N., Bundy, R.M., Al-Subiai, S.N., Barbeau, K.A., Boyle, E.A., 2015. The composition of dissolved iron in the dusty surface ocean: An exploration using size-fractionated iron-binding ligands. Marine Chemistry 173, 125–135.
Gascard, J.-C., et al., 2008. Exploring Arctic Transpolar Drift during Dramatic Sea Ice Retreat. Eos, Trans. Am. Geophys. Union 89 (3), 21–22.
Genovese, C., et al., 2018. Influence of organic complexation on dissolved iron distribution in East Antarctic pack ice. Marine Chemistry 203, 28–37.
Gerringa, L.J., Rijkenberg, M.J., Thuróczy, C.-E., Maas, L.R., 2014. A critical look at the calculation of the binding characteristics and concentration of iron complexing ligands in seawater with suggested improvements. Environ. Chem. 11 (2), 114–136.
Gerringa, L.J.A., Rijkenberg, M.J.A., Schoemann, V., Laan, P., de Baar, H.J.W., 2015. Organic complexation of iron in the West Atlantic Ocean. Mar. Chem. 177, 434–446.
Gledhill, M., Buck, K., 2012. The organic complexation of iron in the marine environment: a review. Front. Microbiol. 3 (69).
Gledhill, M., van den Berg, C.M.G., 1994. Determination of complexation of iron(III) with natural organic complexing ligands in seawater using cathodic stripping voltammetry. Mar. Chem. 47 (1), 41–54.
Gordienko, P.A., Laktionov, A.F., 1969. Section 3.3 - circulation and physics of the Arctic basin waters. In: Gordon, A.L., Baker, F.W.G. (Eds.), Oceanography. Pergamon, pp. 94–112.
Hassler, C.S., Alasonati, E., Mancuso Nichols, C.A., Slaveykova, V.I., 2011. Exopolysaccharides produced by bacteria isolated from the pelagic Southern Ocean — role in Fe binding, chemical reactivity, and bioavailability. Mar. Chem. 123 (1–4), 88–98.
Hassler, C.S., van den Berg, C.M.G., Boyd, P.W., 2017. Toward a regional classification to provide a more inclusive examination of the ocean biogeochemistry of iron-binding ligands. Front. Mar. Sci. 4 (19).
Hogle, S.L., Bundy, R.M., Blanton, J.M., Allen, E.E., Barbeau, K.A., 2016. Copiotrophic marine bacteria are associated with strong iron-binding ligand production during phytoplankton blooms. Limnol. Oceanogr. Lett. 1 (1), 36–43.
Hopwood, M.J., et al., 2018. Non-linear response of summertime marine productivity to increased meltwater discharge around Greenland. Nat. Commun. 9 (1), 3256.
Hudson, R.J.M., Covault, D.T., Morel, F.M.M., 1992. Investigations of iron coordination and redox reactions in seawater using 59Fe radiometry and ion-pair solvent extraction of amphiphilic iron complexes. Mar. Chem. 38 (3), 209–235.
Hunter, K.A., Boyd, P.W., 2007. Iron-binding ligands and their role in the ocean biogeochemistry of iron. 4. pp. 221–232 4.
IPCC, 2014. Climate Change 2014: Synthesis Report. Contribution of Working Groups I, II and III to the Fifth Assessment Report of the Intergovernmental Panel on Climate Change [Core Writing Team, R.K. Pachauri and L.a. Meyer (Eds.)]. IPCC, Geneva, Switzerland, pp. 151.
Kanzow, T., 2017. The Expedition PS100 of the Research Vessel POLARSTERN to the Fram Strait in 2016. 1866-3192.
Klunder, M.B., et al., 2012. Dissolved iron in the Arctic shelf seas and surface waters of the Central Arctic Ocean: impact of Arctic river water and ice-melt. J. Geophys. Res.

117 (C1).
Krembs, C., Eicken, H., Junge, K., Deming, J.W., 2002. High concentrations of exopolymeric substances in Arctic winter sea ice: implications for the polar ocean carbon cycle and cryoprotection of diatoms. Deep-Sea Res. I Oceanogr. Res. Pap. 49 (12), 2163–2181.
Kuma, K., Nishioka, J., Matsunaga, K., 1996. Controls on iron(III) hydroxide solubility in seawater: the influence of pH and natural organic chelators. Limnol. Oceanogr. 41 (3), 396–407.
Laglera, L.M., van den Berg, C.M.G., 2009. Evidence for geochemical control of iron by humic substances in seawater. Limnol. Oceanogr. 54 (2), 610–619.
Laglera, L.M., Battaglia, G., van den Berg, C.M.G., 2011. Effect of humic substances on the iron speciation in natural waters by CLE/CSV. Mar. Chem. 127 (1), 134–143.
Laglera, L.M., et al., 2019a. First quantification of the controlling role of humic substances in the transport of Iron across the surface of the Arctic Ocean. Environ. sci. Technol. 53 (22), 13136–13145.
Laglera, L.M., et al., 2019b. Iron organic speciation during the LOHAFEX experiment: Iron ligands release under biomass control by copepod grazing. J. Mar. Syst. 103151.
Lannuzel, D., Grotti, M., Abelmoschi, M.L., van der Merwe, P., 2015. Organic ligands control the concentrations of dissolved iron in Antarctic Sea ice. Mar. Chem. 174, 120–130.
Laukert, G., et al., 2017. Ocean circulation and freshwater pathways in the Arctic Mediterranean based on a combined Nd isotope, REE and oxygen isotope section across Fram Strait. Geochim. Cosmochim. Acta 202, 285–309.
Lin, H., Twining, B.S., 2012. Chemical speciation of iron in Antarctic waters surrounding free-drifting icebergs. Mar. Chem. 128-129, 81–91.
Liu, X., Millero, F.J., 2002. The solubility of iron in seawater. Mar. Chem. 77 (1), 43–54.
Martin, J.H., Fitzwater, S.E., 1988. Iron deficiency limits phytoplankton growth in the North-East Pacific subarctic. Nature 331 (6154), 341–343.
Mawji, E., et al., 2008. Hydroxamate Siderophores: occurrence and importance in the Atlantic Ocean. Environ. Sci. Technol. 42 (23), 8675–8680.
Measures, C.I., 1999. The role of entrained sediments in sea ice in the distribution of aluminium and iron in the surface waters of the Arctic Ocean. Mar. Chem. 68 (1), 59–70.
Meier, W.N., et al., 2014. Arctic Sea ice in transformation: a review of recent observed changes and impacts on biology and human activity. Rev. Geophys. 52 (3), 185–217.
Middag, R., De Baar, H., Laan, P., Bakker, K., 2009. Dissolved aluminium and the silicon cycle in the Arctic Ocean. Mar. Chem. 115 (3–4), 176–195.
Millero, F.J., Huang, F., Laferiere, A.L., 2002. The solubility of oxygen in the major sea salts and their mixtures at 25°C. Geochim. Cosmochim. Acta 66 (13), 2349–2359.
Mohamed, K.N., Steigenberger, S., Nielsdottir, M.C., Gledhill, M., Achterberg, E.P., 2011. Dissolved iron(III) speciation in the high latitude North Atlantic Ocean. Deep-Sea Res. I Oceanogr. Res. Pap. 58 (11), 1049–1059.
Nielsdóttir, M.C., Moore, C.M., Sanders, R., Hinz, D.J., Achterberg, E.P., 2009. Iron limitation of the postbloom phytoplankton communities in the Iceland Basin. Glob. Biogeochem. Cycles 23 (3).
Norman, L., et al., 2015. The role of bacterial and algal exopolymeric substances in iron chemistry. Mar. Chem. 173, 148–161.
Orellana, M.V., et al., 2003. Tracing the source and fate of biopolymers in seawater: application of an immunological technique. Mar. Chem. 83 (1–2), 89–99.
Paulsen, M.L., et al., 2017. Carbon bioavailability in a high Arctic Fjord influenced by Glacial Meltwater, NE Greenland. Front. Mar. Sci. 4 (176).
Powell, R.T., Wilson-Finelli, A., 2003. Photochemical degradation of organic iron complexing ligands in seawater. Aquat. Sci. 65 (4), 367–374.
Rapp, I., Schlosser, C., Rusiecka, D., Gledhill, M., Achterberg, E.P., 2017. Automated preconcentration of Fe, Zn, Cu, Ni, Cd, Pb, Co, and Mn in seawater with analysis using high-resolution sector field inductively-coupled plasma mass spectrometry. Anal. Chim. Acta 976, 1–13.
Richter, M.E., von Appen, W.J., Wekerle, C., 2018. Does the East Greenland current exist in the northern Fram Strait? Ocean Sci. 14 (5), 1147–1165.
Rijkenberg, M.J.A., et al., 2008. Changes in iron speciation following a Saharan dust event in the tropical North Atlantic Ocean. Mar. Chem. 110 (1), 56–67.
Rijkenberg, M.J.A., Slagter, H.A., Rutgers van der Loeff, M., van Ooijen, J., Gerringa, L.J.A., 2018. Dissolved Fe in the Deep and Upper Arctic Ocean With a Focus on Fe Limitation in the Nansen Basin. 5. pp. 88.
Rudels, B., et al., 2005. The interaction between waters from the Arctic Ocean and the Nordic Seas north of Fram Strait and along the East Greenland Current: results from the Arctic Ocean-02 Oden expedition. J. Mar. Syst. 55 (1), 1–30.
Rudels, B., et al., 2015. Circulation and transformation of Atlantic water in the Eurasian Basin and the contribution of the Fram Strait inflow branch to the Arctic Ocean heat budget. Prog. Oceanogr. 132, 128–152.
Rue, E.L., Bruland, K.W., 1995. Complexation of iron(III) by natural organic ligands in the Central North Pacific as determined by a new competitive ligand equilibration/adsorptive cathodic stripping voltammetric method. Mar. Chem. 50 (1), 117–138.
Ružić, I., 1982. Theoretical aspects of the direct titration of natural waters and its information yield for trace metal speciation. Anal. Chim. Acta 140 (1), 99–113.
Ryan-Keogh, T.J., et al., 2013. Spatial and temporal development of phytoplankton iron stress in relation to bloom dynamics in the high-latitude North Atlantic Ocean. Limnol. Oceanogr. 58 (2), 533–545.
Sato, M., Takeda, S., Furuya, K., 2007. Iron regeneration and organic iron(III)-binding ligand production during in situ zooplankton grazing experiment. Marine Chemistry 106 (3), 471–488.
Schaffer, J., et al., 2017. Warm water pathways toward Nioghalvfjerdsfjorden Glacier, Northeast Greenland. J. Geophys. Res. 122 (5), 4004–4020.
Schlitzer, R., 2018. Ocean Data View.
Schuur, E.A.G., et al., 2015. Climate change and the permafrost carbon feedback. Nature 520, 171.
Slagter, H.A., et al., 2017. Organic Fe speciation in the Eurasian Basins of the Arctic Ocean and its relation to terrestrial DOM. Mar. Chem. 197, 11–25.
Slagter, H.A., Laglera, L.M., Sukekava, C., Gerringa, L.J.A., 2019. Fe-binding organic ligands in the humic-rich TransPolar drift in the surface Arctic Ocean using multiple voltammetric methods. J. Geophys. Res. 124 (3), 1491–1508.
Smith Jr., W.O., Baumann, M.E.M., Wilson, D.L., Aletsee, L., 1987. Phytoplankton biomass and productivity in the marginal ice zone of the. Fram Strait during summer 1984. 92 (C7), 6777–6786.
Swift, J.H., Aagaard, K., 1981. Seasonal transitions and water mass formation in the Iceland and Greenland seas. Deep Sea Research Part A. Oceanogr. Res. Papers 28 (10), 1107–1129.
Thuróczy, C.E., et al., 2010. Speciation of Fe in the Eastern North Atlantic Ocean. Deep-Sea Res. I Oceanogr. Res. Pap. 57 (11), 1444–1453.
Thuróczy, C.-E., et al., 2011. Distinct trends in the speciation of iron between the shallow shelf seas and the deep basins of the Arctic Ocean. 116. pp. C10.
Tomczak, M., Godfrey, J., 2003. Regional Oceanography: An Introduction. Daya, New Delhi, pp. 390.
Topp, R., Johnson, M., 1997. Winter intensification and water mass evolution from yearlong current meters in the Northeast Water Polynya. J. Mar. Syst. 10 (1), 157–173.
van den Berg, C.M.G., 1982. Determination of copper complexation with natural organic ligands in seawater by equilibration with MnO2 I. Theory. Marine Chemistry 11 (4), 307–322.
van den Berg, C.M.G., 1995. Evidence for organic complexation of iron in seawater. Mar. Chem. 50 (1), 139–157.
van den Berg, C.M.G., 2006. Chemical speciation of iron in seawater by cathodic stripping voltammetry with dihydroxynaphthalene. Anal. Chem. 78 (1), 156–163.
Velasquez, I.B., et al., 2016. Ferrioxamine siderophores detected amongst iron binding ligands produced during the remineralization of marine particles. Front. Mar. Sci. 3, 172.
Vraspir, J.M., Butler, A., 2009. Chemistry of marine ligands and siderophores. Annu. Rev. Mar. Sci. 1, 43–63.
Wagener, T., Pulido-Villena, E., Guieu, C., 2008. Dust iron dissolution in seawater: results from a one-year time-series in the Mediterranean Sea. Geophys. Res. Lett. 35 (16).
Wu, J., Boyle, E., Sunda, W., Wen, L.-S., 2001. Soluble and Colloidal Iron in the Oligotrophic North Atlantic and North Pacific. Science 293 (5531), 847–849.